Transition between the ferroelectric and relaxor states in $0.8Pb(Mg_{1/3}Nb_{2/3})O_3$-$0.2PbTiO_3$ ceramics

R. Jiménez,[1] B. Jiménez,[1] J. Carreaud,[2] J. M. Kiat,[2,3] B. Dkhil,[2] J. Holc,[4] M. Kosec,[4] and M. Algueró[1]
[1]*Instituto de Ciencia de Materiales de Madrid, CSIC, Cantoblanco, 28049 Madrid, Spain*
[2]*Laboratoire Structures, Propriétés et Modélisation des Solides, UMR8580-CNRS, École Centrale Paris, Grande Voie des Vignes, 92295 Châtenay-Malabry, France*
[3]*Laboratoire Léon Brillouin, CE Saclay, 91191 Gif-sur-Yvette Cedex, France*
[4]*Institute Jozef Stefan, Jamova 39, 1000 Ljubjlana, Slovenia*
(Received 11 July 2006; published 7 November 2006)

The phase transition between the ferroelectric and relaxor states for $0.8Pb(Mg_{1/3}Nb_{2/3})O_3$-$0.2PbTiO_3$ ceramics with high chemical homogeneity has been studied by measurements of the dielectric and elastic properties as a function of temperature and of thermal expansion. The room temperature ferroelectric phase structure has been studied in ceramics and powdered samples by Rietveld analysis of x-ray diffraction patterns and by ferroelectric hysteresis loops. Results indicate that the material has well defined, different transition and freezing temperatures, such as the transition is between a monoclinic Cm ferroelectric phase and the nonergodic glass state. The transition presents thermal hysteresis, not only in the transition temperature, but in the kinetics. This indicates that a quite sharp slowing down occurs in the temperature interval between 334 and 344 K: the transition temperatures on cooling and heating.

DOI: 10.1103/PhysRevB.74.184106 PACS number(s): 77.84.Dy, 68.35.Rh, 68.60.Bs

I. INTRODUCTION

A lot of attention is currently being paid to the $Pb(Mg_{1/3}Nb_{2/3})O_3$-$PbTiO_3$ (PMN-PT) relaxor-ferroelectric solid solution because of fundamental and applied issues. Phenomena such as the relaxor (R) state, the transformation between the relaxor and ferroelectric (F) states, and the morphotropic phase boundary (MPB) are not well understood yet. Selected compositions are already being used or are under consideration for a range of technologies, such as actuators and ultrasounds. PMN was one of the first relaxors to be reported,[1] and the material on which most of the work to understand the basis of the relaxor state has been done. PMN, as model relaxor, is characterized by a high, strongly dispersive electric polarizability. The dielectric constant shows a broad maximum with temperature of $\sim 20\,000\varepsilon_o$ at 265 K and 1 kHz, which position shifts toward higher temperatures with frequency within a range of 20 K (the so called Curie range) in the typical 100 Hz–1 MHz interval. Below the maximum, the permittivity also shows significant dispersion, permittivity decreasing when frequency increases.[2] No macroscopic phase transition occurs at the Curie range and the overall symmetry remains cubic down to 5 K, though diffuse scattering in x-ray and neutron diffraction has been associated with the presence of nanometer size polar regions within the cubic phase.[3] These polar nanoregions (PNRs) condense at the so called Burn's temperature, T_B, at $\sim$620 K, who first propose their existence from macroscopic measurements.[4] The temperature dependence of the diffuse scattering suggests that the volume fraction of PNRs increase as the temperature is decreased down to a temperature of $\sim$220 K, below which it maintains a constant value.[5] PNRs originate from site disorder and their dynamics are responsible for the relaxor characteristics, yet the actual mechanisms are still under debate.[6] Relaxors have been proposed to be dipolar glasslike systems.[7] In this model, the (interacting) PNRs present thermally activated polarization fluctuations above a freezing temperature, T_f, and evolve to a nonergodic glass state below T_f. Frustration of polar long range order results from competing interactions (random bonds). The freezing temperature is 217 K for PMN (Ref. 8) that is basically the temperature at which the volume fraction of PNRs, saturates. This model has been questioned, and random fields have been proposed to be the origin,[9] or to play a significant role,[10] in the relaxor state. Recently, neutron inelastic scattering experiments have shown the existence of a ferroelectric soft mode above T_B that becomes overdamped below this temperature, as a result of the condensation of PNRs.[11] This lowest energy transverse optic phonon recovers below 220 K, which seems to indicate that a well developed ferroelectric state, though short range, is established below that temperature.[12] The physical meaning of T_f, i.e., whether it is a freezing temperature or a transition temperature, is still unclear. A high enough electric field causes the development of a rhombohedral long range order below a temperature that is field dependent.[13] This ferroelectric phase undergoes a first order phase transition to the *R* state at 213 K during subsequent heating without field.[14] The addition of small amounts of PT shifts the Curie range so as it is at $\sim$313 K for 0.9 PMN–0.1PT.[15] On cooling, this compound presents a spontaneous *R*-*F* transition, also to a rhombohedral phase (F_R, $R3m$ space group), below room temperature (RT).[5] Further addition of PT causes the shift of the *R* state toward higher temperatures, and the F_R phase is stabilized at RT for 0.85 PMN–0.15 PT.[16] The F_R phase was thought to persist for 0.8 PMN–0.2 PT and 0.7 PMN–0.3 PT,[17] up to $\sim$0.65 PMN–0.35 PT, composition at which a morphotropic phase boundary (MPB) with a tetragonal phase (F_T, $4mm$) had been described earlier.[18] However, since the experimental discovery of a *Cm* monoclinic phase in $Pb(Zr,Ti)O_3$ (PZT) at the MPB,[19] several studies on the structure of MPB phases in relaxor-PT systems such as

PMN-PT, $Pb(Zn_{1/3}Nb_{2/3})O_3$-PT (PZN-PT) and $Pb(Sc_{1/2}Nb_{1/2})O_3$-PT (PSN-PT)[20–22] have reported the presence of monoclinic phases (with space groups *Cm* and *Pm*) around the MPB region. In PMN-PT, recent Rietveld analysis of powder XRD data have shown that two monoclinic phases (M_B and M_C with *Cm* and *Pm* space groups, respectively) exist between 0.73 PMN–0.27 PT and 0.65 PMN–0.35 PT, whereas a rhombohedral one was found for compositions with a PT content below 0.27 (Refs. 21 and 23). In contrast with these previous results, a very recent Rietveld study of powder neutron diffraction data for 0.75 PMN–0.25 PT has evidenced the growth of *Cm* monoclinic order (M_B type), from short range to long range, with decreasing temperature from 300 to 80 K.[24] This strong interest for PMN-PT with composition close to the MPB is motivated by the ultrahigh piezoelectricity and strain under the electric field of single crystals along the ⟨001⟩ pseudocubic direction and textured ceramics.[25,26] These materials are under consideration for the new generation of high sensitivity and high power piezoelectric devices.

Many aspects remain unclear in the structural evolution of these materials. A high temperature, ($T > 380$ K), *R* state has been shown to occur in 0.8 PMN–0.2 PT single crystals by neutron scattering experiments. The study also showed the persistence of PNRs up to 650 K, and the development of a rhombohedral distortion at 360 K,[27] in contradiction with more recent high *q*-resolution neutron scattering experiments on 0.8 PMN–0.2 PT single crystals that did not observe any rhombohedral distortion down to 50 K, though a significant broadening of the (220) Bragg peak was observed below 300 K.[28]

We have studied the temperature dependence of some macroscopic properties of this 0.8 PMN–0.2 PT composition on polycrystalline samples of high chemical homogeneity as an alternative means of studying the development of long range polar order. We reported preliminary results on the dielectric and elastic properties that clearly indicated the occurrence of a transformation between relaxor and ferroelectric states above room temperature.[29] This transition shows thermal hysteresis, not only in the temperature but also in the kinetics, which was discussed within the two stages model for the development of ferroelectric long range order in relaxor systems, recently proposed by Ye *et al.*[16] We present here a complete description of the structural, dielectric, and elastic properties and additional thermal expansion measurements that allow the phase transition to be described in detail and reveal aspects not reported before.

II. EXPERIMENTAL

0.8 PMN–0.2 PT ceramic samples were prepared from powders synthesized by mechanochemical activation of oxides, without any excess of PbO and MgO. This has been considered essential for properly controlling composition when addressing fundamental studies in the PMN-PT system.[21] Details can be found in Ref. 30. The technique provides nanometer-scale chemical homogeneity[31] and ceramics with high crystallographic quality.[30] Contamination from the WC:Co milling media was below 50 and 600 ppm of Co and W, respectively. Sintering was carried out at 1473 K for 1 h in a PbO atmosphere. A heating rate of 3 K min^{-1} was used. These conditions allowed ceramics with a grain size of ~4 μm and a low level of porosity (5–8%) to be obtained.[30] Room temperature phases in the ceramics were studied by x-ray diffraction and Rietveld analysis. High resolution x-ray diffraction measurements were carried out with a highly accurate two-axis diffractometer in a Bragg-Brentano geometry with Cu K_β wavelength issued from an 18 kW rotating anode generator. Structural refinements were accomplished with the XND program.[32] Structure of phases were also studied from powders obtained by gentle grinding of the ceramics with a pestle. A thermal treatment at 923 K for 1 h was carried out before structural characterization of both ceramics and powders for relaxing stresses.

Electrical characterization was carried out on ceramic discs on which Ag electrodes had been painted and sintered at 923 K. The dependence of the dielectric permittivity and losses on temperature was measured with a HP 4284A precision LCR meter. In addition to previously reported measurements that were dynamically accomplished at 1 K min^{-1}, static measurements were carried out. Temperature was varied in 2 K intervals between 298 and 475 K along a heating cooling cycle. Stabilization times longer than 30 min were used that provided a temperature stability better than 0.1 K. Forty-eight frequencies between 20 Hz and 1 MHz were scanned at each temperature. Ferroelectric hysteresis loops were also obtained by current integration. Voltage sine waves of 0.1 Hz frequency and amplitudes up to 1000 V were applied by the combination of a synthesizer/function generator (HP 3325B) and a bipolar operational power supply/amplifier (KEPCO BOP 1000 M). Both the current integrator and the software for loop acquisition and analysis were developed at CSIC.

Bending ceramic bars of $12 \times 2 \times 0.35$ mm^3 dimensions were machined for mechanical characterization. The low frequency Young's modulus and mechanical losses were measured as a function of temperature by dynamical mechanical analysis in a three point bending configuration. A stress sine wave of 12 MPa amplitude, superimposed on a static stress of 15 MPa, was applied to the bars. Unlike previously reported measurements that were dynamically accomplished at 3 K min^{-1} at a single frequency of 9 Hz, slower measurements at 0.1 K min^{-1} were carried out at frequencies of 4 and 30 Hz. This technique has been shown to be very suitable for studying phase transitions[33,34] and the dynamics of domain walls in ferroelectrics.[35] Finally, thermal expansion measurements were carried out on the same ceramic bars at 5 K min^{-1} with a constant force applied of 20 mN.

III. RESULTS

We have used the methodology currently used in the Rietveld analysis of MPB compounds. In particular, as in our previous works in PMN-PT (Ref. 20) and PSN-PT (Ref. 22), we have tested many structural models including phase mixing. Agreement factors for the ceramic and powder samples are given in Table I for the more relevant models. Regarding the ceramic, the best Rwp (agreement factor of the fitting on

TABLE I. Agreement factors of the Rietveld analysis of XRD data for 0.8 PMN–0.2 PT ceramics and powders (obtained from the ceramics, i.e., same size).

Sample	Symmetry	R_{wp}	*GoF*	R_{Bragg}
Ceramic	*R*3*m*	6.97	1.44	5.22
	Cm	6.71	1.39	2.73
Powder	*R*3*m*	6.99	1.62	3.67
	Cm	6.94	1.61	3.03
	Pm	8.26	1.92	3.54
	*Bmm*2	6.85	1.47	4.60
	0.18 *R*3*m*+ +0.82*Cm*	6.73	1.56	3.32

the profile pattern) and Gof (ratio ideally equal to one between *R*wp and *R* exp, the latter roughly being a measurement of the data statistic) agreement factors were obtained for a pure monoclinic *Cm* phase or a pure rhombohedral *R*3*m* phase. However, a significantly lower R_{Bragg} (agreement factor on the integrated intensity of the Bragg peaks) was obtained in the case of the *Cm* phase. *R*3*m* and *Cm* phase mixing was also tested but gave poorer R_{Bragg} factor. For the powder sample, the lowest R_{Bragg} was obtained with the pure *Cm* phase whereas a mixing of monoclinic *Cm* (82%) and rhombohedral *R*3*m* (18%) phases gave slightly better *R*wp and *GoF*. Therefore the structure of both PMN–20 PT powders and ceramics can be considered as monoclinic *Cm*, yet the presence of a small amount of rhombohedral phase cannot be completely excluded. No differences in the monoclinic cells (a=5.699 Å), b=5.693 Å, c=4.030 Å, and β =89.88°) between both types of samples could be observed, and values are in good agreement with those reported earlier by Singh and Pandey.[21] It must be noted that whereas the determined monoclinic unit cell is very close to a rhombohedral one, the structure (symmetry) is definitively different. For instance, the polarization in the case of the monoclinic phase is not constrained to lie along a particular axis (as it is in the rhombohedral symmetry) but can rather be along any axis within the monoclinic plane of symmetry. It is also important to emphasize that even if the monoclinic phase gives the best agreement, the thermal factor refined for the Pb atoms remains very large (4.3 Å^2), which indicates (static and/or dynamic) local disordered displacements. This disorder of the Pb-atoms is a well-known feature of lead-based relaxors and is known to play a key role in these systems.[5]

Results of dielectric permittivity as a function of temperature are given in Figs. 1 and 2. Permittivity at 15 frequencies (selected out of the 48 for clarity) measured in static conditions during successive heating and cooling are shown in Fig. 1(a) and 1(b), respectively. On heating, the permittivity presents non-negligible dispersion in the range between RT and 340 K, permittivity decreasing when the frequency is increased. The permittivity then sharply increases between 340 and 350 K in a manner typical of a ferroelectric to paraelectric phase transition. And finally, above 350 K, a clear change to a relaxor-type behavior is observed: dispersion increases and the permittivity presents a broad maximum with temperature that shifts toward higher temperatures with frequency, from 364.5 K at 20 Hz to 373 K at 1 MHz. In contrast, permittivity measured on cooling presents a relaxor behavior down to RT, and a sharp decrease is not observed at any temperature. The thermal hysteresis is better illustrated in the inset of Fig. 1(b) that shows the permittivity at 10 kHz along a heating cooling cycle. The hysteresis is evident in the 320–350 K interval. The temperature dependence of the reciprocal permittivity at 10 kHz along the same cycle is shown in Fig. 2(a). Neither on heating nor on cooling is a Curie-Weiss behavior observed above the temperature of the maximum permittivity of 368 K. On the contrary, the reciprocal permittivity does present a linear behavior below a temperature of 341 and 330 K for heating and cooling, respectively. The same results were obtained when permittivity was dynamically measured at 1 K min^{-1}. The dependence of the temperature of the maximum dielectric permittivity on frequency along with the fit to a Vogel-Fulcher relationship is shown in Fig. 2(b). The freezing temperature, T_f, activation energy, E_g, and characteristic frequency, f_o, obtained from the fit are given in Table II. In this case, data correspond to dynamic measurements at 1 K min^{-1} on cooling, but very

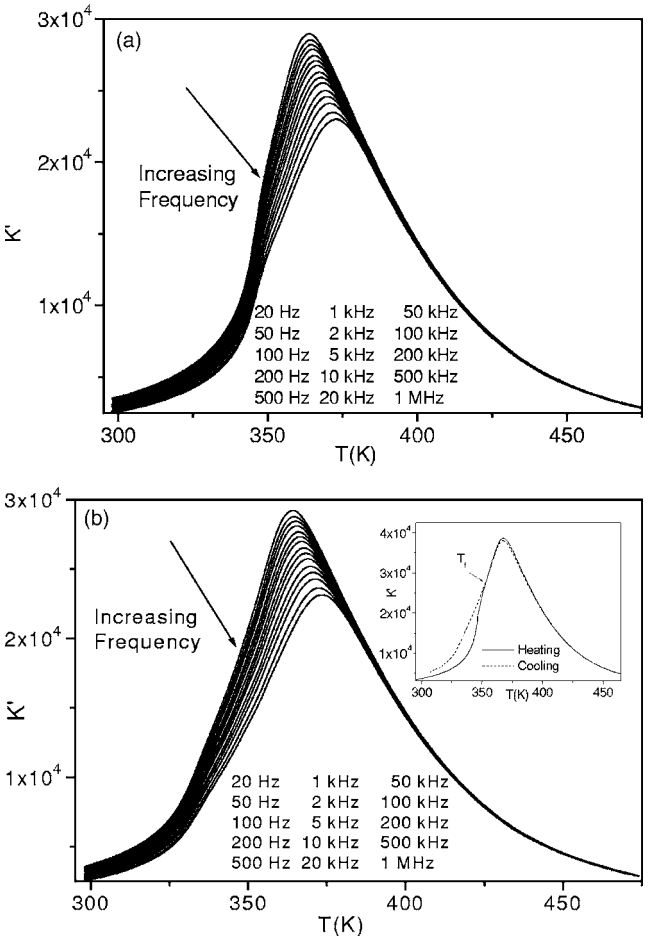

FIG. 1. Dielectric permittivity as a function of temperature at 15 frequencies measured in static conditions during successive (a) heating, and (b) cooling, for a 0.8 PMN–0.2 PT ceramic. The inset in (b) shows the permittivity at 10 kHz along a heating cooling cycle.

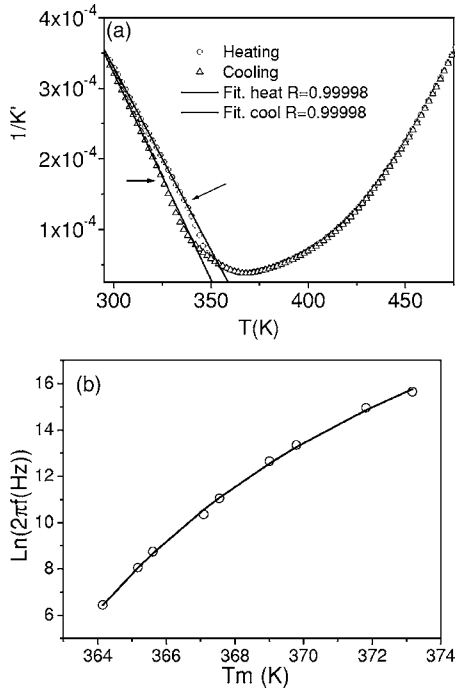

FIG. 2. (a) Temperature dependence of the reciprocal permittivity at 10 kHz along the same cycle of Fig. 1. The regression factors, R, of the linear fits are depicted in the figure, (b) dependence of the temperature of the maximum dielectric permittivity on frequency and fit to a Vogel-Fulcher relationship.

similar parameters were obtained on heating and from static measurements.

Results of the Young's modulus and mechanical losses as a function of temperature are given in Figs. 3 and 4. Differences between the two frequencies measured were not found. Young's modulus decreases with temperature between RT and 344 K, at which it presents a minimum, and then increases. The behavior between RT and 348 K is typical of a ferroelectric to paraelectric phase transition. 348 K is an inflection point, at which the derivative sharply decreases. There is a second inflection point at 358 K, at which the derivative increases again. This second feature was not observed in our previous measurements at 3 K min^{-1}, though it coincides with the temperature at which an amplitude dependence of the Young's modulus vanished.[29] The sharp minimum and inflection points at 344, 348, and 358 K observed during heating do not occur during cooling. Instead, a broad and asymmetric minimum is observed at 334 K. Mechanical losses during heating present a well defined peak at 344 K, which position does not change with the heating rate [see Fig. 2(b)]. The sharp peak is not observed on cooling, but a broad maximum is found at 334 K.

TABLE II. Parameters of the Vogel-Fulcher behavior for the relaxor state in the PMN-PT system.

	T_f (K)	E_a (meV)	F_o (Hz)
PMN[a]	217	79	10^{12}
0.9 PMN–0.1 PT[b]	291	41	1.03×10^{12}
0.8 PMN–0.2 PT[c]	350±2	30	2.5×10^{12}

[a]From Ref. 8.
[b]From Ref. 7.
[c]This work.

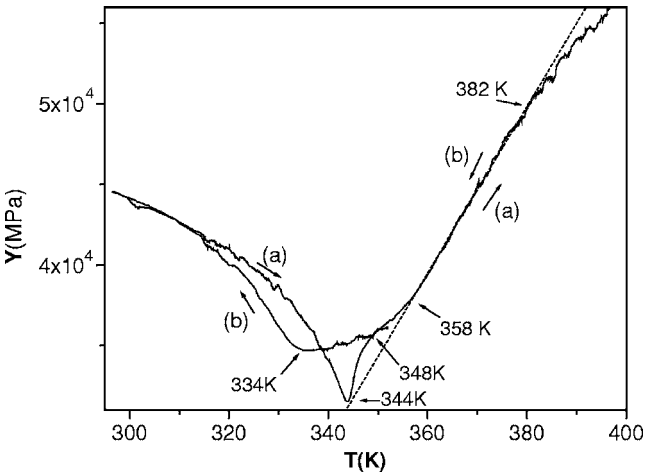

FIG. 3. Young's modulus as a fuction of temperature during successive (a) heating, and (b) cooling, for a 0.8 PMN–0.2 PT ceramic. Minima and inflection points are marked with arrows.

Results of thermal expansion by dilatometry experiments during a heating cooling cycle are shown in Fig. 5. There is a small but sharp contraction at 345 K on heating. Above this temperature, the ceramic maintains a constant dimension until 358 K, from which it starts expanding. There is a clear increase of the derivative at 382 K. Above this point, the derivative keeps slowly increasing and a constant value is reached at 430 K. On cooling, the ceramic contracts with a decreasing derivative until 334 K, where a slight expansion occurs. No inflection points are observed above this temperature.

Finally, a typical room temperature ferroelectric hysteresis loop for these ceramics is shown in Fig. 6. A loop for a 0.7 PMN–0.3 PT ceramic with an analogous microstructure

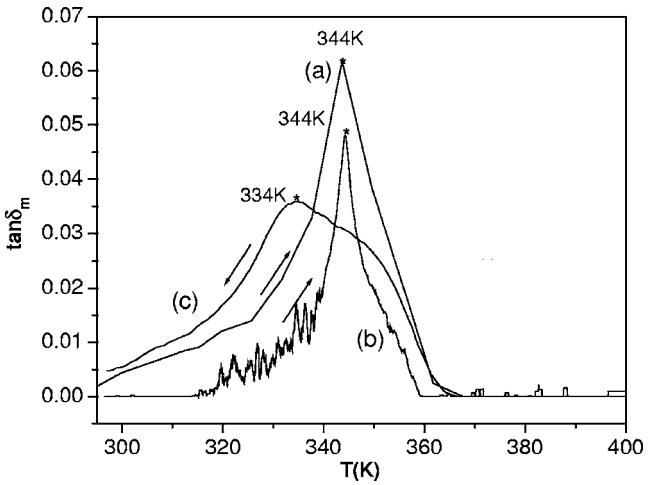

FIG. 4. Mechanical losses as a function of temperature during heating with (a) 2 K min^{-1}, (b) 0.1 K min^{-1} heating rates, and (c) cooling with a −0.1 K min^{-1} rate, for a 0.8 PMN–0.2 PT ceramic. Maxima are marked with stars.

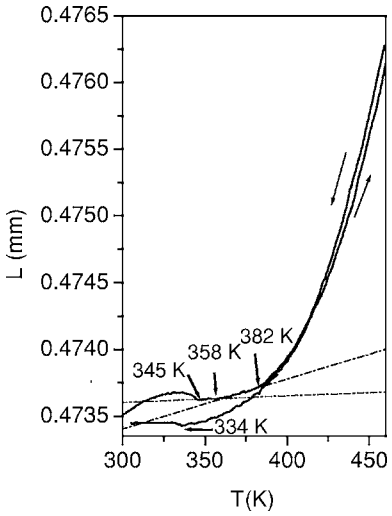

FIG. 5. Dilatometry results during successive heating and cooling for a 0.8 PMN–0.2 PT ceramic. Sharp changes in size and inflection points are marked with arrows.

(grain size and porosity), also processed from powders synthesized by mechanochemical activation, is included for comparison.

It is worth summing up the results on macroscopic properties before the discussion. On heating, the sharp increase of the dielectric permittivity occurs in the temperature range at which the Young's modulus has the minimum and where there is a maximum of mechanical losses (344 K). A contraction occurs at this temperature. The onset of the relaxor type behavior at 350 K occurs at the same temperature than the first inflection point of the Young's modulus. This temperature also corresponds to the freezing temperature T_f obtained from the Vogel-Fulcher relationship. The second inflection point of the Young's modulus at 358 K corresponds to the temperature at which the materials starts expanding after having maintained a constant size from 344 K. There is still a fourth feature at 380 K that only involves the thermal expansion, namely an increase of the derivative. On cooling, in contrast, the broad minimum of the Young's modulus at 334 K occurs at the same temperature at which the material slightly expands.

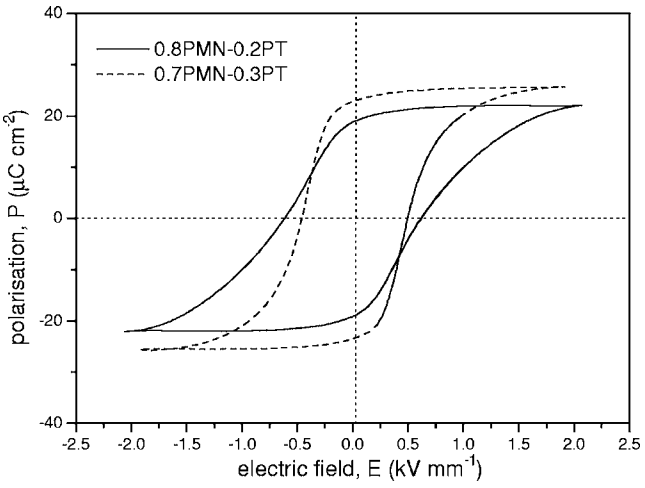

FIG. 6. Ferroelectric hysteresis loops for comparable 0.8 PMN–0.2 PT and 0.7 PMN–0.3 PT ceramics.

TABLE III. Ferroelectric shifts of lead and Mg/Nb/Ti cations in relation to the oxygens barycenter, and polarization (magnitude and direction) calculated with the apparent charges from Hewat (Ref. 36) for the ceramic and powder (obtained from the ceramics, i.e., same size) 0.8 PMN–0.2 PT samples with *Cm* space group.

	Ceramic	Powder
δ Pb-O (Å)	0.30	0.28
δ Ti/Mg/Nb-O (Å)	0.30	0.17
Magnitude (μC/cm^2)	58	48
Direction	[7 7 1]	[5 5 3]

IV. DISCUSSION

Our structural characterization indicates that 0.8 PMN–0.2 PT in the form of both ceramic and powder is monoclinic *Cm*, with the possible presence of a small amount of rhombohedral *R*3*m* phase in the powder. The monoclinic *Cm* structure of morphotropic lead-based compounds can be of two types: M_A type with $P_X=P_Y<P_Z$ components of polarization in the pseudocubic cell, and M_B type with $P_X=P_Y>P_Z$. In order to establish which one is the case for 0.8 PMN–0.2 PT, the magnitude and direction of the macroscopic polarization were calculated as it is currently done in the structural studies of ferroelectric compounds from our structural information by using the formula $P=\frac{e}{V_{cell}}\Sigma_N z''_i \delta i_i$ where e is the charge of the electron, V_{cell} the volume of the unit cell, N the number of ions in the cell, z''_i the apparent charge from Hewat[36] taking into account of the ionic polarization and δi the ionic relative displacement given by structural refinement (see Table III). As Mg, Nb, and Ti cations are, as usual, taken all on the same crystallographic site, an average displacement for the *B* cation is considered. As expected for this composition range of PMN-PT, *Cm* phases in both ceramic and powder are of the M_B type.[21]

These results are consistent with the recent evidence of short-range *Cm* monoclinic order (M_B type) in 0.75 PMN–0.25 PT powder at 300 K, which transforms into a long range M_B phase at 80 K.[24] As a matter of fact, the use of a M_B phase also gave very good agreement factors at 300 K in this latest work, in spite of previous reports of this composition being rhombohedral *R*3*m*.[21] Our results unambiguously show that the monoclinic local order observed in the 0.9 PMN–0.1 PT compound, evidenced by the observation of short range shifts of the Pb^{2+} cations along the ⟨110⟩ directions in addition to the ⟨111⟩ long range rhombohedral shift,[5] has transformed into a long range ordered *Cm* phase for 0.8 PMN–0.2 PT. This transformation of a rhombohedral phase with short ranged monoclinic order toward a long range monoclinic phase was reported for the first time in PMN-PT by Singh and Pandey,[21] though at higher PT contents, and was later also observed in PSN-PT.[22]

The short range monoclinic distortions within a rhombohedral phase were proposed to be the origin of the relaxor-

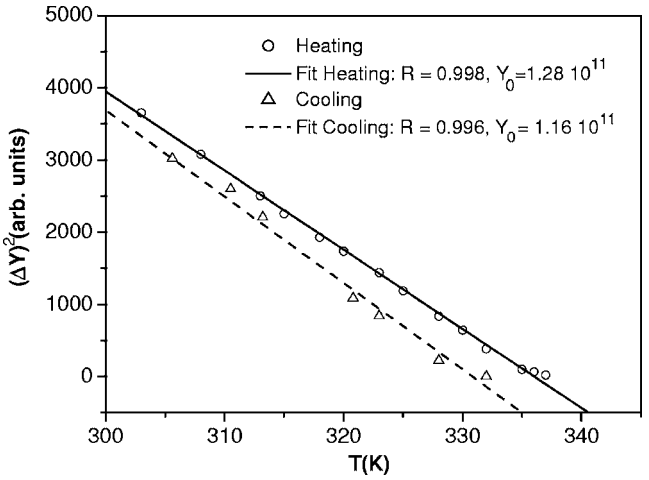

FIG. 7. Temperature dependence of ΔY^2, where $\Delta Y = Y - Y_o$: Y Young's modulus, Y_o the value of the minimum at the transition temperature, in the ferroelectric phase, measured during successive heating and cooling.

type dispersion of the permittivity still present in the ferroelectric phase of 0.9 PMN–0.1 PT.[5] Similar local cationic displacements along the ⟨110⟩ directions exist in rhombohedral $PbZr_xTi_{1-x}O_3$ (Ref. 37), for $0.53 < x < 0.62$ (Ref. 38), and in $Pb(Zn_{1/3}Nb_{2/3})O_3$.[39] These structural characteristics do not only cause permittivity dispersion, but distinctive ferroelectric hysteresis loops. This is also the case for the 0.8 PMN–0.2 PT ceramics reported here. Their ferroelectric loops present smaller polarization and are leant as compared with those for 0.7 PMN–0.3 PT ceramics with the same grain size and porosity, and well developed monoclinic *Cm* long range order.[21] Similar loops have also been observed for 0.75 PMN–0.25 PT single crystals along the ⟨110⟩ direction, and associated with a speckled domain configuration with sizes ranging from 8 μm^2 to less than 100 nm^2.[40]

On heating, the linear dependence of the reciprocal permittivity on temperature suggests that a ferroelectric to paraelectric, second order phase transition is approached. This is the same behavior observed for 0.75 PMN–0.25 PT ceramics.[41] The phase transition can also be studied with the Young's modulus. The mechanical coefficient, Y, is coupled with the electric polarization, P, because of the bilinear interaction mechanoelectric coupling term, ξsP, in the free energy expression, for which ξ is the coupling coefficient and s is the strain. For an isotropic system like a nonpoled ceramic (Ref. 42):

$$Y^2 = \left(\frac{\xi}{s}\right)^2 P^2. \quad (1)$$

Variations of strain in the ferroelectric phase are not large.[16,17] Therefore, the temperature dependence of the Young's modulus is basically due to the dependence of polarization. The temperature dependence of Y^2 on approaching the phase transition from RT is shown in Fig. 7. The increase of modulus, $\Delta Y = Y - Y_o$, where Y_o stands for the value of the minimum at 344 K must be used. A clear linear behavior is found, which indicates that $P^2 \propto (T - T_C)$ on approaching the phase transition as expected for a second order phase transition.

The transition on heating occurs at 344–345 K, the temperature at which the Young's modulus presents a sharp minimum, and where there is a maximum of mechanical losses. These features appear because of the fast decrease of the size of the ferroelectric domains and increase of their number on entering the critical range around the transition, where ferroelectric fluctuations occur. A small but sharp contraction of the material is observed at the transition. The behavior of the permittivity and the Young's modulus are that of a ferroelectric to paraelectric phase transition up to 350 K. However, the material does not linearly expand from 344 to 350 K as one would expect for such a transition, but maintains a constant dimension. This is the same behavior observed for the lattice parameter of 0.8 PMN–0.2 PT single crystals below 380 K,[28] and that was associated with a new X phase, also discussed in $Pb(Zn_{1/3}Nb_{2/3})O_3$-$PbTiO_3$, with an average cubic lattice but ferroelectric polarization.[43,44] At 350 K relaxor-type behavior starts, observed not only in the permittivity, but also in the Young's modulus, for which the derivative sharply decreases as the PNR's start contributing to the mechanical response.[45] The temperature 350 K also corresponds to the freezing temperature. As a matter of fact, the thermal expansion behavior above 344 K is similar to that of a relaxor.[5] All these observations suggest that the material is in a nonergodic glass state in the 344–350 K interval. The transition at 344 K is thus, very likely between a ferroelectric phase and the nonergodic glass state of the relaxor.

The figures for the freezing temperature, activation energy, and characteristic frequency of the relaxor state can be compared with those reported for PMN and 0.9 PMN–0.1 PT that have been included in Table II. Unlike the freezing temperature that increases with the amount of PT in a solid solution, the activation energy decreases when the amount of PT is increased. This activation energy is believed to be the product of an anisotropy energy and the PNR volume.[7] PNR volume has been reported to increase with PT (Ref. 46), so the anisotropy energy must decrease with the addition of PT. Characteristic frequencies of $\sim 10^{12}$ Hz are obtained for the three compositions. There are at least two regimes above the freezing temperature observed on heating. In the first regime, between 350 and 358 K, the PNRs are very mechanically active in the sense that provide a significant softening (a reduction of the Young's modulus). This is the range in which an amplitude dependence has been reported, such as Y decreases when the amplitude of stress increases.[29] This dependence suggests the movement of the PNRs boundaries across the material in this regime.[47] Thermal expansion is negligible, which indicates that the volume fraction of PNRs is constant. In the second regime above 358 K, the softening disappears, and the material starts expanding. These suggest that the volume fraction of PNRs start decreasing and that their dynamics change, so as their boundaries stop moving under stress. There could be a third regime above 380 K, the temperature at which the thermal expansion coefficient sharply increases, though the Young's modulus does not show any inflection point at this temperature.

On cooling, inflection points as those observed on heating at 380, 358, and 350 K are not found. Neither it is observed

a sharp minimum of the Young's modulus nor a sudden decrease of permittivity that shows a relaxor type behavior down to room temperature. Instead, the Young's modulus presents a broad, asymmetric minimum at 334 K, a temperature at which a slight expansion occurs. These suggest that a phase transition to a ferroelectric phase occurs at this temperature. This is further supported by the linear behavior of the reciprocal permittivity and of the squared Young's modulus on cooling [see Figs. 2(a) and 7]. The results indicate that there is a strong thermal hysteresis, not only in the temperature of the transition that is decreased from 345 K to ~334 K, but also in the characteristic time scale of the transition that seems to increase, i.e., in the kinetics that slow down. This hysteretic behavior can be interpreted within the two stages model for the development of ferroelectric long range order in relaxor systems, recently proposed by Ye *et al.*[16] In this model, in a first stage at high temperature, PNRs start condensing at T_d (670 K for 0.8 PMN–0.2 PT).[27] Their number and size increases as the temperature is decreased until approaching the temperature of the phase transition. Then, the second stage begins that is characterized by the onset of ferroelectric fluctuations. As a matter of fact, this picture is confirmed by our results on heating, in which the ferroelectric fluctuations and the relaxor state are successively observed. The model proposes that the kinetics of the transition is controlled by the number of PNRs at the onset of the ferroelectric fluctuations, which depends on temperature. Therefore, the kinetics is slower the lower is the temperature of the transition, and controls the final states. The thermal hysteresis in the characteristic time scale of the transition for 0.8 PMN–0.2 PT would then be a consequence of the hysteresis in the temperature of the transition, and of the transition being slowed down in this interval. The slowing down has been experimentally observed here, and shown to be a quite sharp process that occurs between 334 and 345 K. 0.7 PMN–0.3 PT does not present such hysteresis in the kinetics,[29] for both transition temperatures (402 and 408 K) are above the range of temperatures at which the slowing down occurs, and therefore the macroscopic properties present well defined sharp features at the transition both on heating and cooling. On the other hand, transition temperatures for 0.9 PMN–0.1 PT are below this range, and the kinetics is always slow. As a consequence, the macroscopic properties do not reflect the transition either on heating or on cooling. For PMN, the transition would be extremely slow,[16] and whether a ferroelectric state is established at the end is under debate.[12]

It is worth commenting on the relation between the transition temperature and the freezing temperature. 0.8 PMN–0.2 PT has well defined, independent freezing T_f and transition T_c temperatures, the first being at a high temperature. This means that the ferroelectric phase transforms in a nonergodic glass state on heating, and that ferroelectric long range order does not develop from the relaxor state until the system has frozen. Another issue worth commenting on is the order of the phase transition. We discussed that the temperature dependence of the permittivity and Young's modulus on approaching the transition from the ferroelectric phase indicates second order character. However, the size of the material presents a discontinuity at the transition, and thermal hysteresis is evident, which both rather suggest a first order transition. This apparent contradiction could be related to the nature of the transition that is not either an order disorder or a displacive standard transition, but a transformation between short range and long range polar order. This may be a kind of percolation process of small (short-range order) monoclinic clusters, the PNRs. It must be noted that the R-F transition for 0.7 PMN–0.3 PT is between the relaxor state and the ferroelectric tetragonal phase, which then transforms into the thombohedral one at a lower temperature.[29] This suggest that PNRs are not monoclinic, but tetragonal for this latter composition. We have not discussed the origin of the sharp increase of the thermal expansion coefficient of 0.8 PMN–0.2 PT at 380 K, observed on heating. It is tempting to suggest that it is reflecting the transformation of the monoclinic PNRs into tetragonal ones.

V. CONCLUSIONS

A *Cm* monoclinic phase (of M_B type) has been evidenced for both ceramics and powder of 0.8 PMN–0.2 PT, in agreement with the recent structural characterization of Singh *et al.* for 0.75 PMN–0.25 PT.[24] This long range order monoclinic phase at room temperature may arise from a kind of percolation of small (short-range order) monoclinic clusters occurring at ~334 K. The ceramics present distinctive electrical properties that are most probably associated with the size of the monoclinic domains, which would be then smaller than for comparable 0.7 PMN–0.3 PT ceramics. The ferroelectric phase transforms into a relaxor state on heating. The system has well defined and different transition and freezing temperatures, the latter being the highest, so the transition is always between the ferroelectric phase and the nonergodic glass state of the relaxor. The transition presents thermal hysteresis, not only in the transition temperature, but in the kinetics. This behavior seems to indicate that a quite sharp slowing down occurs in the temperature interval between the transition temperatures on heating and cooling, i.e., between 334 and 344 K.

ACKNOWLEDGMENTS

This research has been funded by MEC through the Project No. MAT2005-01304, and by the EC through the Network of Excellence MIND (Multifunctional and Integrated Piezoelectric devices, Ref. No. E 515757-2).

[1] G. A. Smolenskii and A. I. Agranovskaya, Sov. Phys. Tech. Phys. **3**, 1380 (1958).
[2] L. E. Cross, Ferroelectrics **151**, 305 (1994).
[3] N. de Mathan, E. Husson, G. Calvarin, J. R. Gavarri, A. W. Hewat, and A. W. Morrell, J. Phys.: Condens. Matter **3**, 8159 (1991).
[4] G. Burns and F. H. Dacol, Phys. Rev. B **28**, 2527 (1983).
[5] B. Dkhil, J. M. Kiat, G. Calvarin, G. Baldinozzi, S. B. Vakhrushev, and E. Suard, Phys. Rev. B **65**, 024104 (2002).
[6] W. Kleemann, J. Dec, S. Miga, and R. Pankrath, Ferroelectrics **302**, 493 (2004).
[7] D. Viehland, S. J. Jang, L. E. Cross, and M. Wutting, J. Appl. Phys. **68**, 2916 (1990).
[8] D. Viehland, M. Wutting, and L. E. Cross, Ferroelectrics **120**, 71 (1991).
[9] V. Westphal, W. Kleemann, and M. D. Glinchuk, Phys. Rev. Lett. **68**, 847 (1992).
[10] R. Pirc and R. Blinc, Phys. Rev. B **60**, 13470 (1999).
[11] P. M. Gehring, S. Wakimoto, Z. G. Ye, and G. Shirane, Phys. Rev. Lett. **87**, 277601 (2001).
[12] S. Wakimoto, C. Stock, R. J. Birgeneau, Z. G. Ye, W. Chen, W. J. L. Buyers, P. M. Gehring, and G. Shirane, Phys. Rev. B **65**, 172105 (2002).
[13] H. Arndt, F. Sauerbier, G. Schmidt, and L. A. Shebanov, Ferroelectrics **79**, 145 (1988).
[14] G. Calvarin, E. Husson, and Z. G. Ye, Ferroelectrics **165**, 349 (1995).
[15] S. L. Swartz, T. R. Shrout, W. A. Schulze, and L. E. Cross, J. Am. Ceram. Soc. **67**, 311 (1984).
[16] Z. G. Ye, Y. Bing, J. Gao, A. A. Bokov, P. Stephens, B. Noheda, and G. Shirane, Phys. Rev. B **67**, 104104 (2003).
[17] O. Noblanc, P. Gaucher, and G. Calvarin, J. Appl. Phys. **79**, 4291 (1996).
[18] S. W. Choi, T. R. Shrout, S. J. Jang, and A. S. Bhalla, Ferroelectrics **100**, 29 (1989).
[19] B. Noheda, J. A. Gonzalo, L. E. Cross, R. Guo, S.-E. Park, D. E. Cox, and G. Shirane, Phys. Rev. B **61**, 8687 (2000).
[20] J. M. Kiat, Y. Uesu, B. Dkhil, M. Matsuda, C. Malibert, and G. Calvarin, Phys. Rev. B **65**, 064106 (2002).
[21] A. K. Singh and D. Pandey, Phys. Rev. B **67**, 064102 (2003).
[22] R. Haumont, B. Dkhil, J. M. Kiat, A. Al-Barakaty, H. Dammak, and L. Bellaïche, Phys. Rev. B **68**, 014114 (2003).
[23] A. K. Singh, D. Pandey, and O. Zaharko, Phys. Rev. B **68**, 172103 (2003).
[24] A. K. Singh and D. Pandey, J. Appl. Phys. **99**, 076105 (2006).
[25] S. E. Park and T. R. Shrout, J. Appl. Phys. **82**, 1804 (1997).
[26] E. M. Sabolsky, A. R. James, S. Kwon, S. Trolier-McKinstry, and G. L. Messing, Appl. Phys. Lett. **78**, 2551 (2001).
[27] T. Y. Koo, P. M. Gehring, G. Shirane, V. Kiryukhin, S. G. Lee, and S. W. Cheong, Phys. Rev. B **65**, 144113 (2003).
[28] G. Xu, D. Viehland, J. F. Li, P. M. Gehring, and G. Shirane, Phys. Rev. B **68**, 212410 (2003).
[29] M. Algueró, B. Jiménez, and L. Pardo, Appl. Phys. Lett. **87**, 082910 (2005).
[30] M. Algueró, A. Moure, L. Pardo, J. Holc, and M. Kosec,Acta Mater. **54**, 501 (2006).
[31] M. Algueró, J. Ricote, and A. Castro, J. Am. Ceram. Soc. **87**, 772 (2004).
[32] J. F. Bérar, IUCr. Sat. Meeting on Powder Diffractometry, Toulouse, 1990.
[33] B. Jiménez, A. Castro, and L. Pardo, Appl. Phys. Lett. **82**, 3940 (2003).
[34] R. Jiménez, A. Castro, and B. Jiménez, Appl. Phys. Lett. **83**, 3350 (2003).
[35] M. Algueró, B. Jiménez, and L. Pardo, Appl. Phys. Lett. **83**, 2641 (2003).
[36] A. W. Hewat, Ferroelectrics **6**, 215 (1974).
[37] D. L. Corker, A. M. Glazer, R. W. Whatmore, A. Stallard, and F. Fauth, J. Phys.: Condens. Matter **10**, 6251 (1998).
[38] Ragini, R. Ranjan, S. K. Mishra, and D. Pandey, J. Appl. Phys. **92**, 3266 (2002).
[39] G. Xu, Z. Zhong, Y. Bing, Z. G. Ye, and G. Shirane, Nat. Mater. **5**, 134 (2006).
[40] X. Zhao, J. Y. Dai, J. Wang, H. L. W. Chan, C. L. Choy, X. M. Wan, and H. S. Luo, Phys. Rev. B **72**, 064114 (2005).
[41] A. A. Bokov and Z. G. Ye, Appl. Phys. Lett. **77**, 1888 (2000).
[42] E. K. H. Salje, *Phase Transitions in Ferroelastic and Coelastic Crystals* (Cambridge University Press, Cambridge, 1993).
[43] K. Ohwada, K. Hirota, P. W. Rehrig, Y. Fujii, and G. Shirane, Phys. Rev. B **67**, 094111 (2003).
[44] G. Xu, Z. Zhong, Y. Bing, Z. G. Ye, C. Stock, and G. Shirane, Phys. Rev. B **67**, 104102 (2003).
[45] B. Jiménez and R. Jiménez, Phys. Rev. B **66**, 014104 (2002).
[46] A. D. Hilton, A. Randall, D. J. Barber, and T. R. Shrout, Ferroelectrics **93**, 379 (1989).
[47] A. E. Glazounov, A. K. Tagantasev, and A. J. Bell, Phys. Rev. B **53**, 11281 (1996).